Available Online at www.jourcc.com

Journal homepage: www.JOURCC.com

Journal of Composites and Compounds

Predictive drug release modeling of curcumin from Ag_2O/SiO_2-functionalized CS/PVA/SA hydrogels for enhanced wound healing

Kamran Shirbache [a], ***Ali Shirbacheh*** [b]*

[a] *Hôpital Robert Debré, Groupe Hospitalier Universitaire AP-HP Nord-Université Paris-Cité, France*

[b] *Urgences de Centre Hospitalier de L'agglomération de Nevers, France*

ABSTRACT

Chitosan/poly(vinyl alcohol)/sodium alginate (CS/PVA/SA) hydrogels have been established as a potential drug delivery vehicle for controlled drug release in wound healing applications when formulated with antimicrobial nanoparticles. In this research, we characterize the effect of particle loading (0–20 wt%) of mesoporous Ag_2O/SiO_2 nanoparticle addition on the curcumin drug release from CS/PVA/SA hydrogels. A first-order kinetic model was created to be able to predict drug release from CS/PVA/SA hydrogels with varying Ag_2O/SiO_2 NP composition fractions. The experimental results validated the model well (i.e., global RMSE = 0.0625), demonstrating that drug release is effectively slowed in a substantive manner depending on the nanoparticle loading added. Reliability of the system in the context of parametric uncertainty was evaluated through the use of Monte Carlo Simulations along with the kinetic model, where success probability was defined as the potential to achieve >80% cumulative drug release. Our results demonstrated a significant time-dependent increase in the success probability (R^2 = 0.9822) toward nearly complete certainty after 20 hours, while nanoparticle loading exhibited an inverse relationship on drug release efficiency (R^2 = 1), with the best drug release efficiency occurring at loading below 10wt%. Results offer a way to predictively design nanocomposite hydrogels for personalized drug release applications.

Peer review under responsibility of UGPH.

ARTICLE INFORMATION

Article History:
Received 28 June 2025
Received in revised form 06 September 2025
Accepted 09 September 2025

Keywords:
Monte Carlo simulation
Modeling
Drug release behavior
SiO_2 nanoparticle
Ag_2O nanoparticle
Wound healing

1. Introduction

Hydrogels are three-dimensional polymeric structures that are incapable of dissolving in water, and can absorb significant amounts of biological fluid [1-3]. Hydrogels can be made from both natural and synthetic polymers [4]. Hydrogels are usually classified as either physical, which are held in place by weak secondary forces, or chemical, where stable crosslinked networks are developed through covalent bonds, depending on the interactions that maintain these structures [5, 6]. Swelling behavior, mechanical strength, and biological properties of hydrogels are significant considerations for their structure and morphology [7]. Hydrogels are often used as absorbent, non-adhesive dressings, typically made from either crosslinked gelatin or polysaccharide-based polymers [8].

It is important to understand the wound healing process when developing innovative wound dressing [9, 10]. he human body operates as a highly complex biological system, and cellular mechanisms work together to repair damaged tissues [11]. While healing time often varies with the type of wound and the patient, the biological sequence of repair is similar for all patients. Healing wounds needs to take many factors into consideration, including the choice of an appropriate dressing or ongoing wound care [12].

As one of the innovative wound dressings today, hydrogels made of hydrophilic polymeric materials have demonstrated swelling abilities that create a cooling surface to relieve pain and a moist environment for wound healing [13]. Hydrogels can absorb exudates, facilitate autolytic debridement through hydration, and improve tissue regeneration. Diabetes mellitus is one of the most prevalent chronic metabolic diseases leading to impaired metabolism of carbohydrates, lipids, and proteins due to abnormalities in insulin secretion or sensitivity [14]. This systemic disease can impact multiple organ systems and has several sequalae, including diabetic foot ulcers (DFUs), which are some of the most complex to manage [15]. Ulcers are also attributed to peripheral neuropathy and vascular disease, while skin atrophy decreases the skin's capacity to sustain injury [16]. In addition, loss of pain sensation due to diabetic neuropathy means that many

* *Corresponding author: Ali Shirbacheh, Email: shirbacheh.a@ght58.fr*
https://doi.org/10.61882/jcc.7.3.5

patients are unaware of minor wounds until they are infected, which was found to occur in approximately 15% of patients requiring amputations [17]. Reduced blood circulation and immune response also diminish wound healing [18]. Therefore, it is of increasing importance to generate modern wound dressings that permit healing and administered, controlled drug release [19].

Polymeric systems for local drug delivery based on biocompatible and biodegradable materials have recently gained attention in wound management. Polymeric dressings have been evaluated for the management of wounds including polyurethane sponges, chitosan membranes, hydrocolloids, and alginates. Chitosan, a natural polycationic polysaccharide, derived from the partial deacetylation of chitin [20] has garnered interest for its non-toxic biodegradable, biocompatible, hemostatic role, and antimicrobial properties [21]. Due to these characteristics, chitosan is considered a promising material for drugs delivery systems, and tissue engineering in the field of wound healing.

Several studies have reported the successful incorporation of chitosan in wound dressing systems. Mi et al.[22] developed a bilayer chitosan-based dressing with a dense outer layer and a porous inner layer for the controlled delivery of silver sulfadiazine. Lu et al. [23] synthesized chitosan–nanosilver composite dressings using self-assembly techniques for enhanced antimicrobial performance. Jayakumar et al. [24] and Liu et al. [25] reviewed the applications of chitosan-based hydrogels and drug delivery systems (DDSs) in wound healing. Liang et al. [26] fabricated AgNP/chitosan composites with asymmetric surface wettability, while Ehterami et al. [27] designed insulin-loaded chitosan nanoparticles coated onto electrospun poly(εcaprolactone)/collagen scaffolds. Adeli et al. [28] produced electrospun PVA/chitosan/starch nanofibrous mats, and Amirian et al. [29] developed an injectable hydrogel using amidated pectin and oxidized chitosan through a Schiff-base reaction without chemical crosslinkers.

The rise of antimicrobial activity in metal nanoparticles, specifically those based on silver, has prompted substantial interest in their use for medical applications in terms of biosensing [30, 31], labeling [32], imaging [33], cell separation [34], and infection control [35]. Metal oxide nanoparticles remain an attractive approach due to favorable chemical stability, cost, and functional properties [36]. However, high surface energy would results in aggregation and loss of activity during the course of chemicals processing to produce a metal oxide nanoparticle [37]. If the metal oxide nanoparticle can be encapsulated in a nanoshell or through nanoporous materials, migration and coalescence can be minimized and stability and activity of the nanoparticle maximized [38]. In the case of biomedical applications, an ideal encapsulating matrix would also be chemically inert, biocompatible, non-toxic, and cost-effective. In this regards, silica (SiO2) is a satisfactory encapsulating material as it possesses desirable chemical stability, morphological integrity, non-toxicity, biocompatibility and high porosity [39]. These attributes allow an increased surface interaction and diffusion of the nanoparticle through the silica matrix.

The inhibitive properties of silver nanoparticles, alongside the porous structure of silica, optimize both antimicrobial efficacy and drug release capabilities in hydrogel matrices. Farazin et al. [40], reported silver nanoparticles being stabilized by encapsulation with mesoporous silica to reduce agglomeration and develop surface effectiveness. They proceeded to fabricate and characterize chitosan/poly(vinyl alcohol)/sodium alginate (CS/PVA/SA) hydrogels that were carrying mesoporous AgO_2/SiO_2 and curcumin nanoparticles. The biocompatible and efficient wound dressing system showed improved drug release properties and successfully combined the bioactive properties of curcumin with the antibacterial properties of silver and stability properties of silica.

In this investigation, we explore the impact of different composition fractions of Ag_2O/SiO_2 nanoparticles (NPs) on CS/PVA/SA hydrogels in terms of the controllable drug release behavior. A first-order kinetic model has been established to predict the drug release within hydrogels varying in composition fractions of Ag_2O/SiO_2 NPs. This first order model is then incorporated into the Monte Carlo simulations to evaluate success probability and find good parameter values needed to achieve a targeted drug release profile. These predictive insights will give a procedural framework to optimize hydrogels formulation, which could be beneficial in wound healing applications that requires controlled and sustained drug release to enhance tissue regeneration and infection control.

2. Materials and methods

A first-order kinetic model was developed to describe the drug release behavior of CS/PVA/SA hydrogels of varying composition fractions from Ag_2O/SiO_2 NPs:

$$\frac{M_t}{M_\infty} = A(\varphi)(1 - e^{-k(\varphi)t}) \quad (1)$$

where $\frac{M_t}{M_\infty}$ represents the fraction of drug released at time t, $A(\varphi)$is the maximum release fraction that is also dependent upon fractional composition of Ag_2O/SiO_2 NPs, φ, and $k(\varphi)$ is the release rate constant is also dependent on φ.

Where both $A(\varphi)$ and $k(\varphi)$ are represented as cubic polynomials of φ:

$$A(\varphi) = c_0 + c_1\varphi + c_2\varphi^2 + c_3\varphi^3 \quad (2)$$

$$k(\varphi) = c'_0 + c'_1\varphi + c'_2\varphi^2 + c'_3\varphi^3 \quad (3)$$

c_0, c_1, c_2, c_3, c'_0, c'_1, c'_2, and c'_3 re unknowns that are obtained with the experimental dataset. Once developed, the first order model is combined with Monte Carlo simulation [41] to predict success probability, in order to develop true optimally parameterized values for obtaining desired drug release. This method provides a quantitative understanding of the robustness and reliability of delivery of drug release while also allowing for the design and optimization of controlled release formulations.

3. Results and discussion

In Ref. [40], the drug release behavior of CS/PVA/SA hydrogels containing different composition fractions of Ag_2O/SiO_2 nanoparticles (0, 5, 10, 15, and 20 wt%) was evaluated using an in vitro release study in phosphate-buffered saline (PBS) at pH 7.4. For each formulation, 60 mg of dried hydrogel was immersed in 40 mL of PBS inside an Erlenmeyer flask and placed in an orbital shaker maintained at 37 °C and 300 rpm to simulate physiological conditions. At predetermined time intervals, 5 mL aliquots were withdrawn from each flask and immediately replaced with an equal volume of fresh PBS to maintain sink conditions. The concentration of curcumin released into the medium was quantified using a UV-visible spectrophotometer at its characteristic absorption wavelength. A calibration curve was first established using standard curcumin solutions of known concentrations to correlate absorbance values with drug concentration. The percentage of drug released at each time point was calculated based on the ratio of the amount of curcumin released at time t (C_t) to the initial total amount of curcumin loaded in the hydrogel (C_i), according to the equation:

$$Drug\ Release = \frac{C_t}{C_i} \quad (4)$$

This procedure allowed for a comparative assessment of how varying Ag_2O/SiO_2 nanoparticle content influenced the release kinetics of curcumin from the hydrogel matrix.

In the following, the experimental release profiles of curcumin from hydrogels containing different nanoparticle loadings (0–20 wt%) [40] are successfully fitted using a cubic φ-dependent first-order model:

$$\frac{M_t}{M_\infty} = (0.98 + 0.01\varphi + 0.001\varphi^2 - 0.00007\varphi^3) \times (1 - e^{-(0.29-0.051\varphi+0.003\varphi^2-0.00008\varphi^3)t}) \quad (5)$$

A comparison of the experimental cumulative curcumin release from CS/PVA/SA hydrogels [40] and the curves predicted by the proposed φ-dependent cubic model, is shown in Fig. 1 The model has a global RMSE of 0.0625, demonstrating good agreement for all NP loadings. The drug-release kinetic profiles for hydrogels containing 0, 5, 10, 15, and 20 wt% mesoporous Ag_2O/SiO_2 NPs suggest a clear dependence of the curcumin release process on NP content.

Curcumin released quickly in nanocrystal-free hydrogels (0 wt%), achieving nearly 100% cumulative release (~98%) in 16 hours, which is consistent with burst-release profiles. Increasing the NP content of Ag_2O/SiO_2 NPs resulted in a progressively slower release that became more sustained and balanced; thus, the release increased more slowly. This is largely due to the mesoporous structure of SiO_2 that physically encapsulates curcumin molecules, and intermolecular interactions, for example, hydrogen bonding or adsorption of curcumin to the surface of the nanoparticles or chemistries within the polymer itself. As such, having a larger total NP content led to less total curcumin released, as at least a small fraction of it was being sequestered in phosphorous nanopores and physically in the polymer network itself, during the timescale of the experiment.

It is interesting that while cumulative release was somewhat lower, the hydrogels containing more nanoparticles, especially 20 wt%, exhibited controlled and sustained release kinetics that are desirable traits for long-term therapeutic dosing and improved wound healing. In addition, these outcomes indicate that nanoparticle concentration is a modulating factor and release rates and cumulative drug release can be adjusted by nanoparticle concentration for targeted biomedical applications.

Finally, the developed first order model is integrated with Monte Carlo simulation to assess the success probability, determining optimal parameter values for obtaining desired drug release. Considering the experimental data reported by [40], the *LSF* is defined as:

$$\frac{M_t}{M_\infty} - 0.8 > 0 \quad (6)$$

The coefficient 0.8 is chosen based on the results obtained by Farazin et al. [41]. Considering the uniform probability distribution for composition fractions of Ag_2O/SiO_2 NPs, φ, and time, t, defined within the specified ranges listed in Table 1. Then, by generating 100,000 random values for each measurable variable, the probability of drug release falling within the functional safety region is derived based on the developed model.

Table 1
The range of parameter used in the Monte Carlo simulation [41].

Parameters	Range	
	Minimum value	Maximum value
φ ($wt\%$)	0	20
t (hr)	0	24

The success probability of drug release, defined as the probability of achieving the drug release exceeding 0.8%, was systematically evaluated as a function of both time and the composition fraction of Ag_2O/SiO_2 NPs. As illustrated in Fig. 2a, the release probability exhibits a pronounced time-dependent increase, following a nonlinear polynomial trend ($y = 2E{-}05\ x^6 - 0.002\ x^5 + 0.06\ x^4 - 0.8278\ x^3 + 5.3231\ x^2 - 10.712\ x + 1.2669$, $R^2 = 0.9822$), indicating that the release kinetics are governed by a complex, multi-stage mechanism, likely involving initial lag phase followed by accelerated diffusion or matrix erosion, ultimately reaching near-complete release after approximately 20 hours. On the contrary, Fig. 2b shows a strong inverse relationship between the composition of nanoparticles and the probability of release success, where the fitted curve ($y = -0.0061x^4 + 0.2402x^3 - 2.7297x^2 + 3.4721x + 78.916$, $R^2 = 1$) indicates that release efficiency declines rapidly when the Ag_2O/SiO_2 composition exceeds 10%, potentially due to drug diffusion being impeded from a denser matrix or because the nanoparticles are clumped together, increasing the interactions between the drug molecules and the polymer. There is an important design trade-off to consider as Ag_2O/SiO_2 NPs will provide certain beneficial functions (such as antimicrobial resistance or targeting) but it is important to consider concentrations which do not detract from the overall release goals of the drug itself.

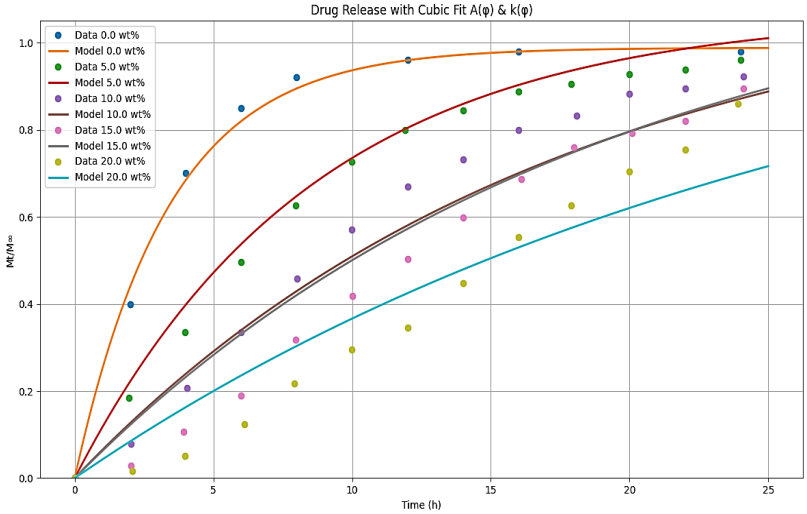

Fig. 1. Drug release behavior of CS/PVA/SA hydrogels with different composition fractions of Ag_2O/SiO_2 NPs.

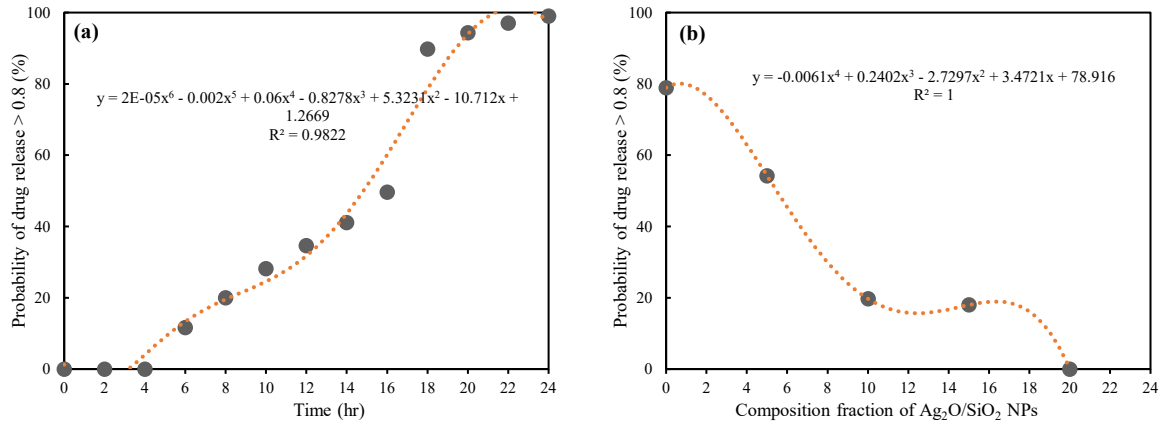

Fig. 2. The success probability of drug release in terms of (a) time, (b) composition fraction of Ag_2O/SiO_2 NPs.

4. Conclusion

This research illustrates that the incorporation of mesoporous Ag_2O/SiO_2 NPs alters the release kinetics of curcumin in a quoted fashion into CS/PVA/SA hydrogels to develop a tunable platform for advanced wound dressings.

A φ-dependent first-order kinetic model was developed to capture how the nanoparticles affect both the quantity and rate of drug release, and experimental data [41] showed good agreement with the statistical model (RMSE = 0.0625). Higher nanoparticle loadings (>10 wt%) exhibited slower release profiles as a result of entrapment within the silica and in the interactions between the nanoparticles and the polymer; however, the higher nanoparticle content associated with decreasing cumulative release of curcumin illustrates the tension between a functional material and therapeutic wisdom. Using a Monte Carlo simulation, it was established that success > 80% release (percentage of drug released) is strongly time-dependent, with a near 100% probability after 20 hours, but inversely dependent on the fraction of the nanoparticle loading, as lower fractions of nanoparticle concentrations showed more success. This work demonstrates a predictive and driven data structure to create optimal formulations of hydrogel nanocomposites which are designed with an appropriate ratio of sustained release of therapeutic use with anti-microbial functionality, which is crucial for the control of complex wounds such as diabetic foot ulcers.

Author contributions

Kamran Shirbache: Investigation, Writing – original draft, Writing – review & editing; **Ali Shirbacheh:** Conceptualization, Writing – original draft, Writing – review & editing.

Funding

No funding was received for this study.

Conflict of interest

The authors declare no conflict of interest.

Data availability

No data is available.

REFERENCES

[1] Y. Yang, H. Chen, X. Zou, X.-L. Shi, W.-D. Liu, L. Feng, G. Suo, X. Hou, X. Ye, L. Zhang, Flexible carbon-fiber/semimetal Bi nanosheet arrays as separable and recyclable plasmonic photocatalysts and photoelectrocatalysts, ACS applied materials & interfaces 12(22) (2020) 24845-24854.
[2] J. Guo, J. Gao, C. Xiao, L. Chen, L. Qian, Mechanochemical reactions of GaN-Al2O3 interface at the nanoasperity contact: Roles of crystallographic polarity and ambient humidity, Friction 10(7) (2022) 1005-1018.
[3] N. Gao, X. Guo, J. Deng, B. Cheng, H. Hou, Elastic wave modulation of double-leaf ABH beam embedded mass oscillator, Applied Acoustics 173 (2021) 107694.
[4] X. Zhu, F. Lin, Z. Zhang, X. Chen, H. Huang, D. Wang, J. Tang, X. Fang, D. Fang, J.C. Ho, Enhancing performance of a GaAs/AlGaAs/GaAs nanowire photodetector based on the two-dimensional electron–hole tube structure, Nano letters 20(4) (2020) 2654-2659.
[5] H. Zheng, B. Zuo, Functional silk fibroin hydrogels: preparation, properties and applications, Journal of Materials Chemistry B 9(5) (2021) 1238-1258.
[6] A.N. Tahneh, B. Dashtipour, A. Ghofrani, S.K. Nejad, Crosslinked natural hydrogels for drug delivery systems, Journal of Composites and Compounds 4(11) (2022) 109-123.
[7] X. Zhang, Y. Zhang, Heat transfer and flow characteristics of Fe3O4-water nanofluids under magnetic excitation, International Journal of Thermal Sciences 163 (2021) 106826.
[8] S. Mondal, S. Das, A.K. Nandi, A review on recent advances in polymer and peptide hydrogels, Soft Matter 16(6) (2020) 1404-1454.
[9] Y. Li, X. Ren, T. Zhao, D. Xiao, K. Liu, D. Fang, Dynamic response of stiffened plate under internal blast: Experimental and numerical investigation, Marine structures 77 (2021) 102957.
[10] N.B. Hoveizavi, F. Alihosseini, S. Lehner, P. Meier, S. Gaan, Colorimetric pH-responsive nanofibrous hydrogels for in vitro monitoring of wound infection, Journal of Materials Chemistry B (2025).
[11] T.S. Welles, J. Ahn, Investigation of the effects of electrochemical reactions on complex metal tribocorrosion within the human body, Heliyon 7(5) (2021).
[12] V. Kanikireddy, K. Varaprasad, T. Jayaramudu, C. Karthikeyan, R. Sadiku, Carboxymethyl cellulose-based materials for infection control and wound healing: A review, International Journal of Biological Macromolecules 164 (2020) 963-975.
[13] Y. Guo, S. Pan, F. Jiang, E. Wang, L. Miinea, N. Marchant, M. Cakmak, Anisotropic swelling wound dressings with vertically aligned water absorptive particles, RSC advances 8(15) (2018) 8173-8180.
[14] H.J. Choi, T. Thambi, Y.H. Yang, S.I. Bang, B.S. Kim, D.G. Pyun, D.S. Lee, AgNP and rhEGF-incorporating synergistic polyurethane foam as a dressing material for scar-free healing of diabetic wounds, RSC advances 7(23) (2017) 13714-13725.
[15] B.D. Texier, A. Ibarra, F. Melo, Optimal propulsion of an undulating slender body with anisotropic friction, Soft Matter 14(4) (2018) 635-642.
[16] A. Ghorbanpour Arani, N. Miralaei, A. Farazin, M. Mohammadimehr, An extensive review of the repair behavior of smart self-healing polymer matrix composites, Journal of Materials Research 38(3) (2023) 617-632.
[17] G. Avashthi, M. Singh, Ultrasound accelerated near-edge functionalized heterogeneous graphene oxide sonocatalyst for surface optical bandwidth efficacy and in situ sonothermocatalysis, New Journal of Chemistry 45(12) (2021) 5463-5483.
[18] Y.J. Kang, Simultaneous measurement of blood pressure and RBC aggregation by monitoring on–off blood flows supplied from a disposable air-compressed pump, Analyst 144(11) (2019) 3556-3566.

[19] L. Xiao, W. Ni, X. Zhao, Y. Guo, X. Li, F. Wang, G. Luo, R. Zhan, X. Xu, A moisture balanced antibacterial dressing loaded with lysozyme possesses antibacterial activity and promotes wound healing, Soft Matter 17(11) (2021) 3162-3173.
[20] J.L. Shamshina, Chitin in ionic liquids: historical insights into the polymer's dissolution and isolation. A review, Green Chemistry 21(15) (2019) 3974-3993.
[21] M. Salehi, M. Mirhaj, N.B. Hoveizavi, M. Tavakoli, N. Mahheidari, Advancements in Wound Dressings: The Role of Chitin/Chitosan-based Biocomposites, Journal of Composites and Compounds 7(23) (2025).
[22] F.L. Mi, Y.B. Wu, S.S. Shyu, J.Y. Schoung, Y.B. Huang, Y.H. Tsai, J.Y. Hao, Control of wound infections using a bilayer chitosan wound dressing with sustainable antibiotic delivery, Journal of Biomedical Materials Research: An Official Journal of The Society for Biomaterials, The Japanese Society for Biomaterials, and The Australian Society for Biomaterials and the Korean Society for Biomaterials 59(3) (2002) 438-449.
[23] S. Lu, W. Gao, H.Y. Gu, Construction, application and biosafety of silver nanocrystalline chitosan wound dressing, Burns 34(5) (2008) 623-628.
[24] R. Jayakumar, M. Prabaharan, P.S. Kumar, S. Nair, H. Tamura, Biomaterials based on chitin and chitosan in wound dressing applications, Biotechnology advances 29(3) (2011) 322-337.
[25] H. Liu, C. Wang, C. Li, Y. Qin, Z. Wang, F. Yang, Z. Li, J. Wang, A functional chitosan-based hydrogel as a wound dressing and drug delivery system in the treatment of wound healing, RSC advances 8(14) (2018) 7533-7549.
[26] D. Liang, Z. Lu, H. Yang, J. Gao, R. Chen, Novel asymmetric wettable AgNPs/chitosan wound dressing: in vitro and in vivo evaluation, ACS applied materials & interfaces 8(6) (2016) 3958-3968.
[27] A. Ehterami, M. Salehi, S. Farzamfar, A. Vaez, H. Samadian, H. Sahrapeyma, M. Mirzaii, S. Ghorbani, A. Goodarzi, In vitro and in vivo study of PCL/COLL wound dressing loaded with insulin-chitosan nanoparticles on cutaneous wound healing in rats model, International journal of biological macromolecules 117 (2018) 601-609.
[28] H. Adeli, M.T. Khorasani, M. Parvazinia, Wound dressing based on electrospun PVA/chitosan/starch nanofibrous mats: Fabrication, antibacterial and cytocompatibility evaluation and in vitro healing assay, International journal of biological macromolecules 122 (2019) 238-254.
[29] J. Amirian, Y. Zeng, M.I. Shekh, G. Sharma, F.J. Stadler, J. Song, B. Du, Y. Zhu, In-situ crosslinked hydrogel based on amidated pectin/oxidized chitosan as potential wound dressing for skin repairing, Carbohydrate Polymers 251 (2021) 117005.
[30] Y.-B. Hahn, R. Ahmad, N. Tripathy, Chemical and biological sensors based on metal oxide nanostructures, Chemical Communications 48(84) (2012) 10369-10385.
[31] N.B. Hoveizavi, M. Laghaei, S. Tavakoli, B. Javanmardi, Wearable biosensors incorporating nanocomposites: advancements, applications, and future directions, Journal of Composites and Compounds 6(21) (2024).
[32] L. Cheng, S. Shen, D. Jiang, Q. Jin, P.A. Ellison, E.B. Ehlerding, S. Goel, G. Song, P. Huang, T.E. Barnhart, Chelator-free labeling of metal oxide nanostructures with zirconium-89 for positron emission tomography imaging, ACS nano 11(12) (2017) 12193-12201.
[33] D.W. Moon, Y.H. Park, S.Y. Lee, H. Lim, S. Kwak, M.S. Kim, H. Kim, E. Kim, Y. Jung, H.-S. Hoe, Multiplex protein imaging with secondary ion mass spectrometry using metal oxide nanoparticle-conjugated antibodies, ACS Applied Materials & Interfaces 12(15) (2020) 18056-18064.
[34] H. Xu, Z.P. Aguilar, L. Yang, M. Kuang, H. Duan, Y. Xiong, H. Wei, A. Wang, Antibody conjugated magnetic iron oxide nanoparticles for cancer cell separation in fresh whole blood, Biomaterials 32(36) (2011) 9758-9765.
[35] M. Alavi, M. Rai, Topical delivery of growth factors and metal/metal oxide nanoparticles to infected wounds by polymeric nanoparticles: an overview, Expert Review of Anti-infective Therapy 18(10) (2020) 1021-1032.
[36] L. Chen, Z. Liu, Z. Guo, X.-J. Huang, Regulation of intrinsic physicochemical properties of metal oxide nanomaterials for energy conversion and environmental detection applications, Journal of Materials Chemistry A 8(34) (2020) 17326-17359.
[37] K. Mondal, A. Sharma, Recent advances in electrospun metal-oxide nanofiber based interfaces for electrochemical biosensing, RSC advances 6(97) (2016) 94595-94616.
[38] J. Deng, P. Ren, D. Deng, L. Yu, F. Yang, X. Bao, Highly active and durable non-precious-metal catalysts encapsulated in carbon nanotubes for hydrogen evolution reaction, Energy & Environmental Science 7(6) (2014) 1919-1923.
[39] P. Xiang, K. Petrie, M. Kontopoulou, Z. Ye, R. Subramanian, Tuning structural parameters of polyethylene brushes on silica nanoparticles in surface-initiated ethylene “living” polymerization and effects on silica dispersion in a polyolefin matrix, Polymer Chemistry 4(5) (2013) 1381-1395.
[40] A. Farazin, M. Mohammadimehr, A.H. Ghasemi, H. Naeimi, Design, preparation, and characterization of CS/PVA/SA hydrogels modified with mesoporous Ag 2 O/SiO 2 and curcumin nanoparticles for green, biocompatible, and antibacterial biopolymer film, RSC advances 11(52) (2021) 32775-32791.
[41] M. Mohammadi, M. Khamehchi, Y. Li, Modeling and Monte Carlo simulation of dye-sensitized solar cells based on TiO2/g-C3N4 nanocomposites, Journal of Power Sources 646 (2025) 237313.